Published in final edited form as:
Exp Hematol. 2013 August ; 41(8): . doi:10.1016/j.exphem.2013.04.002.

A model of glucose-6-phosphate dehydrogenase deficiency in the zebrafish

Xiaobai Patrinostro, **Michelle L. Carter**, **Ashley C. Kramer**, and **Troy C. Lund**
Division of Pediatric Blood and Marrow Transplant, University of Minnesota, Minneapolis, Minnesota, USA

Abstract

Glucose-6-phosphate dehydrogenase (G6PD) deficiency is the most common genetic defect and enzymopathy worldwide, affecting approximately 400 million people and causing acute hemolysis in persons exposed to prooxidant compounds such as menthol, naphthalene, anti-malarial drugs, and fava beans. Mouse models have not been useful because of a lack of significant response to oxidative challenge. We turned to zebrafish (*Danrio rerio*) embryos, which develop ex utero and are transparent, allowing visualization of hemolysis. We designed morpholinos to zebrafish *g6pd* that were effective in reducing gene expression as shown by Western blot and G6PD enzyme activity, resulting in a brisk hemolysis and pericardial edema secondary to anemia. Titration of the *g6pd* knockdown allowed us to generate embryos that displayed no overt phenotype until exposed to the prooxidant compounds 1-naphthol, menthol, or primaquine, after which they developed hemolysis and pericardial edema within 48–72 hours. We were also able to show that *g6pd* morphants displayed significant levels of increased oxidative stress compared with controls. We anticipate that this will be a useful model of G6PD deficiency to study hemolysis as well as oxidative stress that occurs after exposure to prooxidants, similar to what occurs in G6PD-deficient persons.

Glucose-6-phosphate dehydrogenase (G6PD) deficiency is one of the most common genetic enzyme defects in the world, with a possible 400 million cases. The lack of G6PD causes a decline in the amount of nicotinamide adenine dinucleotide phosphate (NADPH) and a decrease in reduced glutathione (GSH). NADPH and GSH are the only molecules with which red blood cells can metabolize free radicals produced by prooxidative drugs and cellular processes. The result of G6PD deficiency is a propensity for an individual to develop hemolysis when exposed to prooxidant compounds; these include sulfonamide antibiotics, antimalarials, and fava beans [1]. Neonates who are G6PD deficient are at an increased risk of hyperbilirubinemia caused by excessive erythrocyte lysis within 24 hours of delivery. Hyperbilirubinemia can lead to kernicterus and, if untreated, can lead to lifelong neurologic disabilities [2]. In addition, children exposed to mothballs containing naphthalene or camphor can develop acute hemolysis. Finally, children with malaria receiving antimalarials (prototypically primaquine) can develop G6PD deficiency–triggered hemolysis that can result in life-threatening anemia [3,4]. These latter two groups of patients reside mostly in low-income countries; particularly sub-Saharan Africa where up to 20% of

Offprint requests to: Troy C. Lund, MMC 366, University of Minnesota, 420 Delaware Street SE, Minneapolis, MN 55455 USA; lundx072@umn.edu.

Supplementary data related to this article can be found online at http://dx.doi.org/10.1016/j.exphem.2013.04.002.

Author contributions: X.P., M.L.C., A.C.K. performed the experiments; T.C.L. performed the data analysis and wrote the manuscript.

Conflict of interest disclosure
No financial interest/relationships with financial interest relating to the topic of this article have been declared.

persons may be G6PD deficient [5,6]. Because G6PD is located on the X chromosome, the majority of the clinical hemolytic crises occur in males, but G6PD deficiency is so common in some countries that females can also suffer from hemolysis and neonatal hyperbilirubinemia [7].

In the past, mouse models for G6PD deficiency have been limited by early embryonic death because of disease severity or conversely displayed poor sensitivity to oxidative stress [8,9]. A new model developed by the Fok lab may have overcome some of these barriers, although distribution is limited [10]. The zebrafish is increasing in popularity as a model for human disease [11–13]. Some of the early developmental work in zebrafish was in the modeling of hematopoiesis, particularly in the genetic causes of anemia. Several fish models have been created with specific mutations leading to reductions in hematopoietic stem cells or display alterations in specific hematopoietic linages (reviewed by Davidson et al. [12]). Zebrafish models have also been created to study various biological aspects of erythrocytes including iron transport, erythrogenesis, and spherocytosis [14–16].

We sought to create a new vertebrate model of G6PD deficiency using the zebrafish, which has a single gene for *g6pd* which has homology to the mammalian form. We used morpholinos (MOs) targeted to the 5-prime exons of *g6pd* to transiently knockdown its expression. We were able to induce a profound anemia after *g6pd* knockdown that resulted in significant pericardial edema. Titration of the amount of MO used to attenuate *g6pd* expression allowed us to determine a level of *g6pd* gene expression in morphants that displayed no overt phenotype until exposed to prooxidant compounds such as menthol, 1-naphthol, or the prototypical antimalarial drug primaquine. We show that these drugs can elicit a prooxidant condition in zebrafish. The resulting phenotype from drug exposure and *g6pd* deficiency was one of hemolysis leading to cardiac edema, shown by reduced hemoglobin staining and a reduction in the number of erythroblasts when we used a *Tg(gata1: DsRed)* transgenic fish line in similar experiments. This vertebrate model could may help us to understand more of the pathophysiologic processes associated with oxidative stress and G6PD deficiency and perhaps help to determine pathways or agents that might alleviate oxidative stress for clinical applications.

Methods

Zebrafish strains and fish husbandry

Fish were maintained by the University of Minnesota Zebrafish Core Facility according to standardized procedures [17] and with the approval of the International Animal Care and Use Committee. Wild type fish were obtained from Segrest Farms (Gibsonton, FL, USA) and bred in-house. Other fish strains maintained in-house used include *Tg(gata1:DsRed)sd2* [18].

Morpholino

The *g6pd* antisense translation blocker and splice MOs were designed and purchased from Gene Tools (Philomath, OR, USA). The MOs were dissolved in water at a stock concentration of 0.1 mmol/L. Various amounts of MO were delivered via air pressure injected into one- to two-cell–stage embryos in volumes of 3–6 nL volumes. The *g6pd* MOs were combined in a 1:1 ratio for delivery of 1.4 or 1.2 pmol as indicated in the results. Random MOs at 1.4 or 1.2 pmol were used for control injection. The *g6pd* translation blocking the MO sequence was 5’-gcgctcgctcgactgcc-catcattt-3’; the splice-blocking MO sequence was 5’-ataataaaa-gacttaccgaagcgccc-3’. The random MO was created with a similar GC content and random bases used. Random MOs from three different batches were used.

The gene for *Danio rerio g6pd* was cloned downstream into the pCR4-TOPO (Invitrogen, Grand Island, NY, USA) and RNA produced by in vitro transcription from the T7 promoter using the Ambion mMessage Machine Kit (Life Technologies, Grand Island, NY, USA) followed by purification using the Ambion Megaclear Kit (Life Technologies). For RNA rescue experiments, 30 pg of RNA was injected into one- to two-cell–stage embryos.

Western blot

Single-cell embryos were injected with increasing amounts of MO. At 72 hours post fertilization (hpf), 20 embryos were frozen in a pellet. The embryo pellet was thawed and lysed with rapid lysis buffer containing 2.5% 2-mercaptoethanol (Invitrogen). One cycle of freeze thawing in liquid nitrogen was then performed. Next, one-quarter volume of 4× lithium dodecyl sulfate sample buffer (Invitrogen) was added. Embryos were vortexed briefly and boiled for 8 min, and debris was pelleted by centrifugation before loading SDS-polyacrylamide gels for electrophoresis and transfer of protein to PVDF membrane according the manufacturer's instructions (Invitrogen). The blot was blocked in phosphate-buffered saline (PBS) containing 1% Tween-20 and 5% blocking reagent (Bio-Rad, Hercules, CA, USA) overnight. Anti-G6PD (ab87230; Abcam, Cambridge, MA, USA) in blocking buffer was incubated with the membrane for 2 hours at room temperature. The appropriate secondary antibody was then used for primary antibody detection (goat anti-rabbit conjugated to horseradish peroxidase, sc-2004; Santa Cruz Biotechnology, Santa Cruz, CA, USA). The blot was developed via chemiluminescence according to the manufacturer's protocol (GE-Amersham, Pittsburgh, PA, USA) and scanned on a flatbed scanner.

G6pd enzyme activity

The G6pd activity assay was performed as described previously [19]. Ten zebrafish embryos at 72 hpf were pelleted and snap frozen in liquid nitrogen. Protein was extracted and G6pd the reaction was performed using 100 mL of Tris-based buffer containing 1% saponin as described previously [19] at room temperature for 10 min. Next, 10 mL of the extract was blotted to 1MM Whatman paper and allowed to dry at room temperature. Fluorescence was determined by excitation under an ultraviolet light (360 nm), and the image was captured using an AlphaImager (ProteinSimple, San Jose, CA, USA) with a yellow filter.

Staining and imaging

Hemoglobin staining was performed as described previously [20]. Dechorionated live embryos at 72 hpf were stained in 0.6 mg/mL o-dianisidine (Sigma-Aldrich, St. Louis, MO) containing 0.01 mol/L sodium acetate (pH 4.5), 0.65% H_2O_2, and 40% ethanol in the dark for 15 min. Embryos were then dehydrated through graded ethanol washes of 50%, 75%, and 100%, for 5 min each. Finally, embryos were cleared in benzyl benzoate and benzyl alcohol at a 2:1 ratio. Embryos were stored in the clearing solution until imaged using a Leica M165FC fluorescent microscope with PlanAPO 1.6×/0.05 NA objective (Leica Camera Inc., Allendale, NJ, USA). Image capture was performed with Leica LAS software, and postprocessing was performed using Adobe Photoshop CS4 (Mountain View, CA, USA). Dark field images of 96 hpf embryos were taken using a QImaging Retiga 2000R camera and QCapture software on an inverted Leica DMI6000B microscope with a 5× objective. Hemoglobin quantification was obtained by importing color images into ImageJ (http://rsbweb.nih.gov/ij/) followed by processing using a color deconvolution plugin to extract o-dianisidine staining of the ventral cardiac region. Images were then converted to greyscale and pixel density was quantified, followed by calculation of the mean and SEM.

Reactive oxygen species assays

Dechorionated 72-hpf embryos were incubated in chloromethyl-2',7'-dichlorodihydrofluorescein diacetate (CM-H2DCFDA; Invitrogen, catalog no. C6827) at a concentration of 500 ng/mL in embryo water for 2–2.5 hours at 28.5°C and protected from light. Embryos were then placed in a Constar black, opaque, flat-bottom plate, one embryo per well, in 200 mL of embryo water plus dye per well. Fluorescence was read with a BioTek (Winooski, VT) Synergy2 microplate reader using the BioTek Gen5 software. Software settings were: 485/20 excitation, 528/20 emission, 100% sensitivity, 50% upper reading, and probe set 4 mm above the well.

Hydroethidine was purchased from Polysciences (Warrington, PA, USA). Hydroethidine was resuspended in dimethylsulfoxide, aliquoted into single-use stocks, and stored under nitrogen in the dark at 4°C. Ten 72-hpf zebrafish embryos were digested with 1 mL of prewarmed 0.25% Trypsin-EDTA in Dulbecco modified Eagle medium (DMEM; Invitrogen) for 10 min at room temperature. Trypsin was deactivated by 1 mL of prewarmed 10% fetal bovine serum in DMEM. Samples were then triturated with a P1000 pipet and filtered through a 40-μm filter into polycarbonate tubes, pelleted, washed once with PBS, and spun down again. Cells were resuspended in 2 μmol/L of hydroethidine solution in PBS and incubated at 32°C, 5% O_2, 4.2% CO_2 for 30 min. After incubation, samples were pelleted and washed once with PBS and resuspended in 300 μL of PBS and analyzed on a BD FACSCanto flow cytometer (BD Biosciences, San Jose, CA, USA) using a 488-nm laser line for excitation and gating on dye emission using the 575/26-nm bandpass filter.

Prooxidant exposure

All zebrafish embryos were dechorionated at 24 hpf before drug treatment. 1-Naphthol was obtained from Sigma-Aldrich (catalog no. N1000) and dissolved in 100% ethanol to make a 20 mg/mL concentrated stock. Next, the 1-Naphthol solution was diluted to 10 μg per 5mL, 20 μg per 5 mL and 30 μg per 5 mL in zebrafish embryo water for treatment. Fresh 1-naphthol concentrated stock was made for each experiment, and treatment lasted 24–72 hpf. Ethanol diluted to the same concentration was used in control experiments, and embryos never showed any effects. Primaquine bisphosphate was obtained from Sigma-Aldrich (catalog no. 160393) and dissolved in zebrafish embryo water to make a 10 mg/mL concentrated stock. Next, primaquine solution was diluted to 250–400 μg per 5 mL in zebrafish embryo water for treating 24-hpf embryos. Fresh primaquine concentrated stock was made for each experiment, and treatment lasted from 24 hpf to 6 days post fertilization (dpf). Menthol crystals were obtained from Sigma-Aldrich (catalog no. 15785) and dissolved in 100% ethanol for a 1 mol/L stock. The 1-mol/L menthol solution was diluted to either 1:5000 (200 μmol/L) or 1:5500 (181 μmol/L) concentrations in 5 mL of zebrafish embryo water for treatment of embryos from 24 to72 hpf.

Flow cytometry

Tg(gata1:DsRed)sd2 zebrafish embryos at either 72 hpf or 5 dpf (for naphthol or primaquine experiments, respectively) were washed with 1× PBS, incubated with 1 mL of prewarmed 0.25% Trypsin-EDTA (Invitrogen) for 10 min at room temperature and then trypsin inactivated with 10% fetal bovine serum in DMEM. After trypsin inactivation, embryos were triturated to dissociate the cells, filtered through a 40-μm filter, and pelleted at 1000 × g for 5 min. Finally, the cells were washed with 1× PBS, pelleted again, and resuspended in 300 μL of 1× PBS before flow cytometry.

In situ hybridization

The zebrafish *hbbe1.1* gene was purchased from Source BioScience LifeSciences (Nottingham, UK) and subcloned into the pSPT19 vector, followed by in vitro transcription using a SP6/ T7 Transcription Kit (Roche, Indianapolis, IN, USA) according to the manufacturer's instructions. Whole-mount in situ hybridization was performed as described previously [21].

Results

The expression of *Danio rerio g6pd* has been little studied, but it is known to be expressed at any early stage in development in a manner consistent with other housekeeping genes [22]. Our first search for the genomic location of *g6pd* showed it to be located on linkage group 23 per the Zv9 annotated genome in the Ensembl database (http://www.ensembl.org/Danio_rerio/Info/Index). Although much of the zebrafish genome has undergone a duplication event during its evolution [23], we found only a single copy of the *g6pd* gene annotated. The human G6PD gene is located on the X chromosome. Unlike mammals, zebrafish do not have sex chromosomes, and their sex determination mechanisms are not well understood [24]. We found that the closest gene to *g6pd* was *naa10*, a gene coding for an acetyltransferase involved in posttranslational modification. Interestingly, this gene is also closely linked to human *G6PD* on the X chromosome, suggesting some conserved synteny (Fig. 1A). The remainder of the region surrounding *g6pd* on linkage group 23 did not share further synteny. We next compared the amino acid homology of human and zebrafish G6pd and found a 70% similarity between the two proteins, as shown in Figure 1B. We were not surprised to see this high degree of homology because G6pd is part of the fundamental metabolic pathways that were formed early in evolution and are necessary for life.

To knock down *g6pd* expression in the zebrafish, we used MOs designed to target either the start codon or a splice site located between exons 3 and 4. Preliminary experiments showed that when each MO was used alone, there was no phenotypic evidence of *g6pd* knockdown and embryos appeared normal (data not shown). It was only when the MOs were used together that we found 47% of the injected animals ($p < 0.0001$) developed severe cardiac edema and kidney edema at 72 hpf, while random MOs had little effect (Fig. 2). We were able to partially rescue this phenotype with the coinjection of zebrafish *g6pd* messenger RNA (mRNA), indicating 47% affected versus 15% in rescued embryos ($p = 0.0005$). Knowing that severe edema can be the result of erythrocyte hemolysis, we next stained embryos with o-dianisidine to identify hemoglobin-producing erythrocytes followed by quantification. We found a 70% reduction ($p < 0.001$) in the amount of hemoglobin-producing cells in the g6pd morphants versus the control injections at 72 hpf (Fig. 2C and 2D). Next, to confirm that we were indeed having an effect of G6pd protein levels, we performed a Western blot that showed a reduction in G6pd protein (Fig. 3). We also performed a G6pd enzymatic activity assay based on the fluorescent spot assay first described by Beutler et al. [19], which is established on the production of the fluorescent product NAPDH by G6pd activity and is performed on whole-cell lysates. We found a marked reduction in G6pd activity (Fig. 3B). These data suggest that we have effectively knocked down G6pd protein and function using MOs in zebrafish.

Children and adults with G6PD deficiency might have chronic hemolysis depending on their level of enzyme activity [25]. More commonly, they have absent to minimal hemolysis until exposed to a prooxidant, and the susceptibility to hemolysis correlates to the amount of G6PD activity that they retain. To mimic this situation, we lowered the dose of MO to 1.2 pmol (total dose), which still knocked down G6pd protein as shown by Western blot (Fig. 3A), and few animals had significant cardiac edema or hemolysis; when they did develop

anemia, it was of a much milder phenotype. We used this lower dose for all experiments in which prooxidant drugs were tested.

A common trigger that causes hemolysis in children with G6PD deficiency is exposure to mothballs containing naphthalene as an active ingredient. The molecular structure of naphthalene is that of fused benzene rings, which is a reactive intermediate in many chemical reactions. When we treated *g6pd* morphants with naphthalene, we found minimal signs of hemolysis or phenotype (data not shown). Realizing that naphthalene is converted to an active prooxidant metabolite, 1-naphthol, by the liver's CYP450 pathway [26] and that the embryonic zebrafish is just starting to produce a liver outgrowth around 72 hpf [27], we reasoned that exposure to 1-naphthol could be much better at producing a state of oxidative stress. To verify that 1-naphthol was able to induce oxidative stress in the embryos through the production of free radicals, we used dichlorodihydroflourescein diacetate (H_2DCFDA), which is a nonfluorescent compound until cleaved by esterases activated by free radical production within cells; this serves as a general marker of oxidative stress–induced free radical production. Figure 4 shows that we were able to produce a significant oxidative challenge in wild type embryos exposed to 1-naphthol at the lowest dose tested (10 μg; p = 0.007), and oxidative stress slightly increased with the next higher doses (20 and 30 μg). We next evaluated oxidative stress by the use of hydroethidine, a redox-sensitive indicator that allows the intracellular detection of superoxide production and can be evaluated by flow cytometry [28]. Our data show a significant increase in cells having superoxide production at the two highest doses of 1-naphthol (1.7% ± 0.5% the control group; 9.0% ± 3.3% in the 20-μg treatment group; 8.8% ± 2.7% in the 30-μg treatment group; p = 0.03 and 0.01, respectively). The super-oxide induction was particularly significant when a flow cytometry gating strategy enriching for erythrocytes was performed (4.7% ± 0.7% the control group; 28.4% ± 11.4% in the 20-μg treatment group; 28.3% ± 10.4% in the 30-μg treatment group; p = 0.03 and 0.02, respectively). These results demonstrate that 1-naphthol can generate a prooxidant condition in exposed embryos; however, when exposed to the highest dose of 1-naphthol, wild type zebrafish displayed no deficiencies in erythrocyte o-dianisidine staining, indicating that they were able to metabolize the oxidative challenge (Fig. 4D).

We next exposed *g6pd* morphants to 1-naphthol, which showed a significant increase in the amount of free radical production using H_2DCFDA as a fluorescent indicator (Fig. 5). Furthermore, we found that *g6pd* morphants exposed to 1-naphthol had significant hemolysis and cardiac edema compared with random MO-injected embryos, and hemoglobin staining by o-dianisidine was dramatically reduced (Fig. 5). We also noted that there was dose responsiveness to 1-napthol as an increase in dose increased the number of *g6pd* morphants with severe edema. In contrast, random morphants showed much less edema and edema was of a much milder phenotype, even at the highest dose of 1-naphthol. Although significant oxidative stress and hemolysis were seen in *g6pd* morphants as a group, not every embryo displayed an edematous phenotype. To determine whether there were higher levels of reactive oxygen species (ROS) production in those morphants with edema compared to those without edema, we separated morphants based on edematous phenotype and performed the ROS detection assays with H_2DCFDA as before. We found that g6pd morphants with edema had significantly higher levels of ROS than those without (Supplementary Figure E1, online only, available at www.exphem.org).

It is possible that *g6pd* morphants exposed to 1- naphthol were downregulating hemoglobin production instead on undergoing hemolysis. Therefore, we performed MO knockdown and 1-naphthol exposure in *gata1:DsRed* transgenic embryos, which have DsRed-labeled erythroblasts that can be quantified by flow cytometry (Fig. 6). The flow cytometric analysis after *g6pd* knockdown and 1-naphthol exposure showed a significant reduction in DsRed-positive cells at the 10-and 20-μg concentrations of 1-naphthol. There were 55% ± 12.8%

DsRed cells in the 10-μg treatment group and 55% ± 27.3% DsRed cells in the 20-μg treatment group ($p = 0.04$ and 0.05, respectively, when compared with random MO-injected embryos). To indeed verify that apoptosis was occurring versus a downregulation of DsRed or other spurious phenomenon, we stained DsRed-positive erythroblasts from 1-naphthol–treated *g6pd* morphants with annexin–fluorescein isothiocyanate (FITC) followed by flow cytometry using an ImageStream (Amnis, Seattle, WA, USA) flow cytometer, which is able to capture live images of stained cells as they travel through the flow-cell. Cells costaining for both DsRed and annexin-FITC indicated that ongoing apoptosis and hemolysis was occurring in the *g6pd* morphants exposed to 1-naphthol (Fig. 6C). We also performed in situ hybridization for the embryonic globin gene *hbbe1.1*, which is one of the few embryonic globin genes to be active from 15 through 72 hpf [29]. Staining for *hbbe1.1* mRNA was present in normal distribution in control, random, and *g6pd* morphants (Supplementary Figure E2, online only, available at www.exphem.org). There was attenuation in total cell numbers staining for *hbbe1.1* in *g6pd* morphants exposed to 1-naphthol, although the anatomic distribution of stained cells was normal. Exposure to 1-naphthol did not appreciably affect random morphants. These results suggest a mild effect of increased ROS on globin gene transcription, but the reduction in o-dianisidine–staining cells found in our G6pd-deficient embryos most likely occurs through hemolysis predominantly. We cannot rule out the possibility that the transcription of other embryonic globin genes could be affected.

A significant proportion of the sub-Saharan population is afflicted with malaria and rates of G6PD deficiency approach 20% in some countries [1]. Many of the antimalarial compounds used in malaria treatment are significant prooxidants and are triggers of hemolysis in G6PD-deficient individuals [4]. Therefore, we performed experiments using the prototypical antimalarial primaquine to induce oxidative stress as might be seen in the clinical setting. The use of primaquine in our system yielded increased oxidative stress as indicated by H_2DCFDA fluorescence (Fig. 7), and *g6pd* morphants showed significant cardiac edema and reduced hemoglobin staining upon exposure to primaquine ($p < 0.0001$). Unlike 1-naphthol–induced hemolysis, the edema and hemolysis occurred 3 days later at 6–7 dpf, indicating a difference in the timing of the hemolytic process. We were also able to show a reduction in *gata1* expressing (DsRed positive) erythroblasts by performing similar experiments as before using *gata1:DsRed* transgenic embryos. The *g6pd* morphants exposed to primaquine had 58% ± 42% DsRed cells compared with untreated embryos ($p = 0.03$, compared with random morphants). These experiments show that primaquine can induce oxidative stress–driven hemolysis in our model system, similar to the clinical scenario of antimalarial-induced hemolytic anemia in patients who are G6PD deficient.

Finally, it is well described that mothers in some West African countries apply menthol to their children as a healing or well-being ointment or powder. Menthol has strong prooxidant properties [30]. Our testing of menthol applied to *g6pd* morphants showed that we could successively induce hemolysis and massive cardiac and kidney edema, whereas a minimal effect was seen in random MO-injected embryos (Supplementary Figure E3, online only, available at www.exphem.org). These data show that a third classic trigger of oxidative stress–induced hemolysis produced similar results in our system.

Discussion

We have described the first model of G6pd deficiency in the zebrafish. The zebrafish is a rapidly growing model for human disease, especially for diseases affecting the hematopoietic system. The zebrafish has benefits as a model organism because the cost per animal is low versus other vertebrates, and the clutch sizes are much higher, with parental fish producing up to 50–100 offspring per day. The ability to suppress gene expression using

MOs makes it a good model for studying the effects of genetic dysregulation early in life. The genetic program for determination of the blood lineages is conserved in the zebrafish, allowing experiments in erythropoiesis to give insight into mechanisms and pathways that are relevant in higher organisms [12].

We have capitalized on these advantages by knocking down the function of *g6pd* in the zebrafish. The homology of G6pd to other invertebrates is highly conserved. This homology is not unexpected, because many of the enzymes in metabolic pathways are ancestrally conserved and essential for cellular function. The conversion of glucose-6-phosphate to 6-phsophogluconolactone by G6PD is the first step in the pentose phosphate pathway (also termed the *hexose monophosphate shunt*), and it is important in the generation of NADPH, an important coenzyme and reducing agent in lipid and nucleic acid synthesis. NADPH is also important in intracellular redox hemostasis to reduce free radicals. Most of the redox reactions occur in the cytoplasm of cells that are assisted by other pathways in the mitochondria and nucleus. The exceptional case is the red blood cell lacking both mitochondria and a nucleus and relying solely on G6PD and the pentose phosphate pathway for NADPH production [1]; this specifically allows the erythrocyte to be highly susceptible to increased oxidative stress when deficient in G6PD.

The unusual aspect of the fish erythrocyte that must be appreciated is that they contain a nucleus and mitochondria. Other species with a similar phenotype are avian, amphibian, and reptile. It is not known how metabolically active these two organelles are in the erythrocyte, but one could assume that there is some contribution to cellular metabolism. Despite the presence of these organelles, we were able to show a dose-dependent knockdown of G6pd in the zebrafish using an MO-targeted approach. We also found that two targeted MOs (a start codon inhibitor and a splice-blocker) were more effective than a single MO, and this combination allowed us to overcome any actively produced *g6pd*. Further work is ongoing to produce a germ line *g6pd* knockout using genomic engineering techniques.

The phenotype we observed is one of pericardial and, occasionally, renal edema. This edematous phenotype is most likely due to the hemolytic process that we provoked by applying a prooxidant drug treatment in the context of G6pd deficiency. Zebrafish hematopoiesis occurs in successive waves, with the primitive wave of erythroid progenitors arising first as part of the paraxial mesoderm followed by their migration to the midtrunk region, after which they exit into the yolk sac just before the initiation of circulation [20]. This process is followed by the definitive waves of hematopoiesis that begin with erythromyeloid progenitors arising in the posterior blood island [31]. It is interesting to compare our model to other models that lack the production of primitive erythrocytes. For example, the *bloodless* zebrafish does not develop primitive erythrocytes, but can survive to 5 dpf, after which time erythrocytes from the definitive wave of hematopoiesis begin to accumulate to allow the animal to survive to adulthood without ill effects [32]. Another model, *vlad tepes*, has a *gata1* mutation, lacks primitive hematopoiesis, and does not survive beyond 14 dpf. Edema is not an apparent part of the phenotype of these models. These findings are in contrast to a recent model of porphyria in the zebrafish (*montalcino*), which undergoes rapid hemolysis upon exposure to bright light [33]. This model is similar to ours in that the embryos have hemoglobinstaining erythrocytes at 48 hpf, but after light-induced hemolysis they develop acute and significant pericardial edema. These observations show that *bloodless* fish with mutations in the early developmental pathways of erythropoiesis behave much differently than do models that initially produce primitive erythrocytes followed by acute hemolysis. One might speculate that perhaps the circulation of free heme after hemolysis has a significant role in the pathophysiology leading to the cardiac and renal edema observed. It is also well known that free heme accelerates free radical production, which is counterbalanced by heme oxygenase (HO-1) production, which serves to detoxify

free heme [34]. In fact, HO-1 induction has been shown to serve a protective role in ischemic renal failure in some model systems [35].

We describe first zebrafish G6PD deficiency model. In our system, the exposure of classic prooxidants: 1-naphthol, primaquine, and menthol induced brisk hemolysis resulting in significant cardiac (and sometime kidney) edema. This model will be helpful in understanding not only the processes surrounding G6PD deficiency-induced hemolysis, but also genetic dysregulation surrounding oxidative stress. The system we have developed gives a reliable and efficient readout of oxidative stress-induced pathophysiology. In addition, capitalizing on the ability to use fluorescent transgenic zebrafish with various cell lineages marked (e.g., neutrophils, dendritic cells, lymphocytes), we will be able to understand further the effects that oxidative stress has on the development of other hematopoietic cell lineages. Finally, because this system has a rapid and robust readout, there is the possibility of developing a medium-throughput screen for compounds or biological agents with antioxidant activity.

Supplementary Material

Refer to Web version on PubMed Central for supplementary material.

Acknowledgments

This work was supported by the Children's Cancer Research Fund. M.L.C. was supported by National Institutes of Health grant T32 CA099967.

References

1. Cappellini MD, Fiorelli G. Glucose-6-phosphate dehydrogenase deficiency. Lancet. 2008; 371:64–74. [PubMed: 18177777]
2. Hansen TW. Prevention of neurodevelopmental sequelae of jaundice in the newborn. Dev Med Child Neurol. 2011; 53(Suppl 4):24–28. [PubMed: 21950390]
3. Youngster I, Arcavi L, Schechmaster R, et al. Medications and glucose-6-phosphate dehydrogenase deficiency: an evidence-based review. Drug Safety. 2010; 33:713–726. [PubMed: 20701405]
4. Beutler E, Duparc S. Glucose-6-phosphate dehydrogenase deficiency and antimalarial drug development. Am J Trop Med Hyg. 2007; 77:779–789. [PubMed: 17978087]
5. Carter N, Pamba A, Duparc S, Waitumbi JN. Frequency of glucose-6-phosphate dehydrogenase deficiency in malaria patients from six African countries enrolled in two randomized anti-malarial clinical trials. Malaria J. 2011; 10:241.
6. Soghoian S, Nyadedzor C, Ed Nignpense B, Clarke EE, Hoffman RS. Health risks of using mothballs in Greater Accra, Ghana. Trop Med Int Health. 2011; 17:135–138. [PubMed: 21967193]
7. Riskin A, Gery N, Kugelman A, Hemo M, Spevak I, Bader D. Glucose-6-phosphate dehydrogenase deficiency and borderline deficiency: association with neonatal hyperbilirubinemia. J Pediatr. 2012; 161:191–196. [PubMed: 22459229]
8. Wilmanski J, Villanueva E, Deitch EA, Spolarics Z. Glucose-6-phosphate dehydrogenase deficiency and the inflammatory response to endotoxin and polymicrobial sepsis. Crit Care Med. 2007; 35:510–518. [PubMed: 17205013]
9. Longo L, Vanegas OC, Patel M, et al. Maternally transmitted severe glucose 6-phosphate dehydrogenase deficiency is an embryonic lethal. EMBO J. 2002; 21:4229–4239. [PubMed: 12169625]
10. Ko CH, Li K, Li CL, et al. Development of a novel mouse model of severe glucose-6-phosphate dehydrogenase (G6PD)-deficiency for in vitro and in vivo assessment of hemolytic toxicity to red blood cells. Blood Cells Mol Dis. 2011; 47:176–181. [PubMed: 21839656]
11. Novoa B, Figueras A. Zebrafish: model for the study of inflammation and the innate immune response to infectious diseases. Adv Exp Med Biol. 2012; 946:253–275. [PubMed: 21948373]

12. Davidson AJ, Zon LI. The “definitive” (and “primitive”) guide to zebrafish hematopoiesis. Oncogene. 2004; 23:7233–7246. [PubMed: 15378083]
13. Poss KD, Keating MT, Nechiporuk A. Tales of regeneration in zebrafish. Dev Dyn. 2003; 226:202–210. [PubMed: 12557199]
14. De Domenico I, Vaughn MB, Yoon D, Kushner JP, Ward DM, Kaplan J. Zebrafish as a model for defining the functional impact of mammalian ferroportin mutations. Blood. 2007; 110:3780–3783. [PubMed: 17726163]
15. Liao EC, Paw BH, Peters LL, et al. Hereditary spherocytosis in zebrafish riesling illustrates evolution of erythroid beta-spectrin structure, and function in red cell morphogenesis and membrane stability. Development. 2000; 127:5123–5132. [PubMed: 11060238]
16. Ransom DG, Haffter P, Odenthal J, et al. Characterization of zebrafish mutants with defects in embryonic hematopoiesis. Development. 1996; 123:311–319. [PubMed: 9007251]
17. Westerfield, M. The zebrafish book: a guide for the laboratory use of zebrafish (Brachydanio rerio). Eugene, Ore: M. Westerfield; 1993.
18. Traver D, Paw BH, Poss KD, Penberthy WT, Lin S, Zon LI. Transplantation and in vivo imaging of multilineage engraftment in zebrafish bloodless mutants. Nat Immunol. 2003; 4:1238–1246. [PubMed: 14608381]
19. Beutler E, Mitchell M. Special modifications of the fluorescent screening method for glucose-6-phosphate dehydrogenase deficiency. Blood. 1968; 32:816–818. [PubMed: 4386875]
20. Detrich HW 3rd, Kieran MW, Chan FY, et al. Intraembryonic hematopoietic cell migration during vertebrate development. Proc Natl Acad Sci USA. 1995; 92:10713–10717. [PubMed: 7479870]
21. Kozlowska K, Kostulak A, Zurawska-Czupa B. ADCC against hamster transplantable melanoma cells in relation to the diversity of their cell surface. Neoplasma. 1988; 35:503–510. [PubMed: 3063982]
22. McCurley AT, Callard GV. Characterization of housekeeping genes in zebrafish: male-female differences and effects of tissue type, developmental stage and chemical treatment. BMC Mol Biol. 2008; 9:102. [PubMed: 19014500]
23. Postlethwait JH. The zebrafish genome in context: ohnologs gone missing. J Exp Zool B Mol Dev Evol. 2007; 308:563–577. [PubMed: 17068775]
24. Liew WC, Bartfai R, Lim Z, Sreenivasan R, Siegfried KR, Orban L. Polygenic sex determination system in zebrafish. PloS One. 2012; 7:e34397. [PubMed: 22506019]
25. Glucose-6-phosphate dehydrogenase deficiency. Vol. 67. Bull World Health Organ: 1989. WHO Working Group; p. 601-611.
26. Preuss R, Angerer J, Drexler H. Naphthalene–an environmental and occupational toxicant. Int Arch Occup Env Health. 2003; 76:556–576. [PubMed: 12920524]
27. Chu J, Sadler KC. New school in liver development: Lessons from zebrafish. Hepatology. 2009; 50:1656–1663. [PubMed: 19693947]
28. Zhao H, Kalivendi S, Zhang H, et al. Superoxide reacts with hydroethidine but forms a fluorescent product that is distinctly different from ethidium: potential implications in intracellular fluorescence detection of superoxide. Free Radic Biol Med. 2003; 34:1359–1368. [PubMed: 12757846]
29. Brownlie A, Hersey C, Oates AC, et al. Characterization of embryonic globin genes of the zebrafish. Dev Biol. 2003; 255:48–61. [PubMed: 12618133]
30. Olowe SA, Ransome-Kuti O. The risk of jaundice in glucose-6-phosphate dehydrogenase deficient babies exposed to menthol. Acta Paediatr Scand. 1980; 69:341–345. [PubMed: 7376859]
31. Bertrand JY, Kim AD, Violette EP, Stachura DL, Cisson JL, Traver D. Definitive hematopoiesis initiates through a committed erythromyeloid progenitor in the zebrafish embryo. Development. 2007; 134:4147–4156. [PubMed: 17959717]
32. Liao EC, Trede NS, Ransom D, Zapata A, Kieran M, Zon LI. Non-cell autonomous requirement for the bloodless gene in primitive hematopoiesis of zebrafish. Development. 2002; 129:649–659. [PubMed: 11830566]
33. Dooley KA, Fraenkel PG, Langer NB, et al. Montalcino: A zebrafish model for variegate porphyria. Exp Hematol. 2008; 36:1132–1142. [PubMed: 18550261]

34. Kumar S, Bandyopadhyay U. Free heme toxicity and its detoxification systems in human. Toxicol Lett. 2005; 157:175–188. [PubMed: 15917143]

35. Akagi R, Takahashi T, Sassa S. Fundamental role of heme oxygenase in the protection against ischemic acute renal failure. Jap J Pharmacol. 2002; 88:127–132. [PubMed: 11928711]

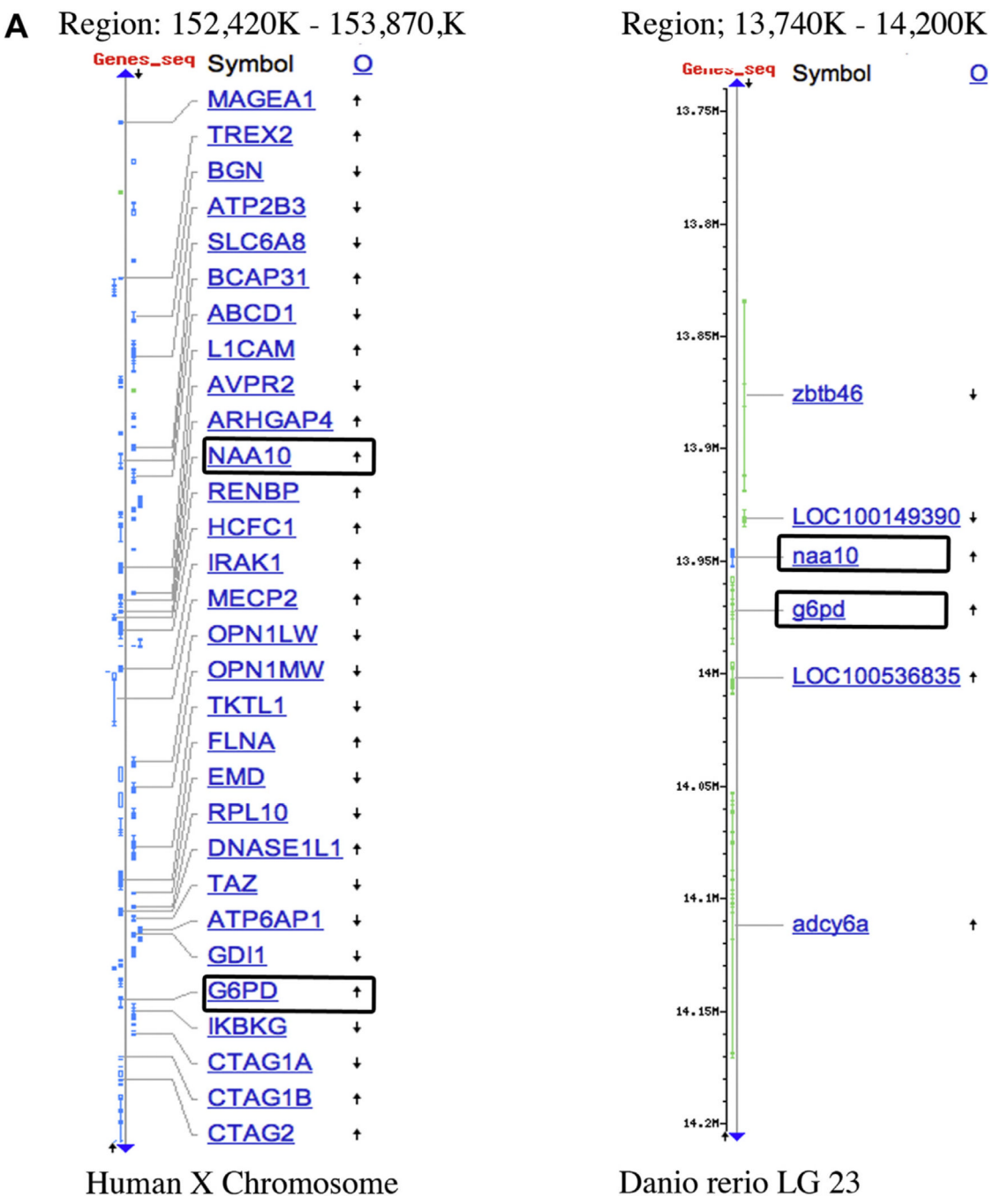

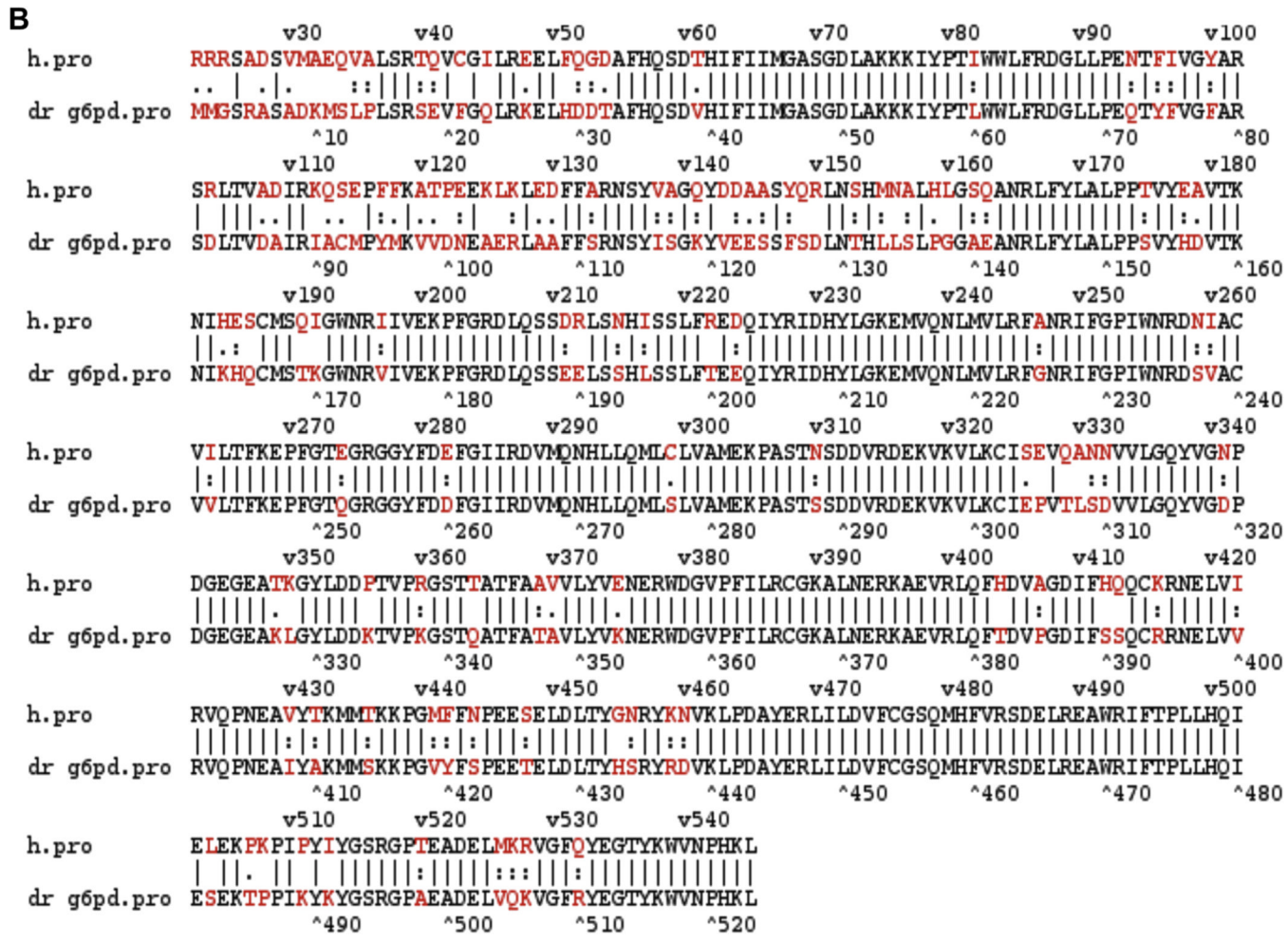

Figure 1.

Location and homology of *Danio rerio g6pd*. **(A)** Genetic linkage map of human chromosome X and the D. *rerio* linkage group 23. Both charts were generated using the NCBI Map Viewer (http://www.ncbi.nlm.nih.gov/mapview/). Boxed genes show synteny. **(B)** Amino acid homology between human G6PD and D. *rerio* G6pd proteins using protein MegAlign alignment software following the Lipman-Pearson pairwise algorithm from DNAStar (Madison, WI, USA).

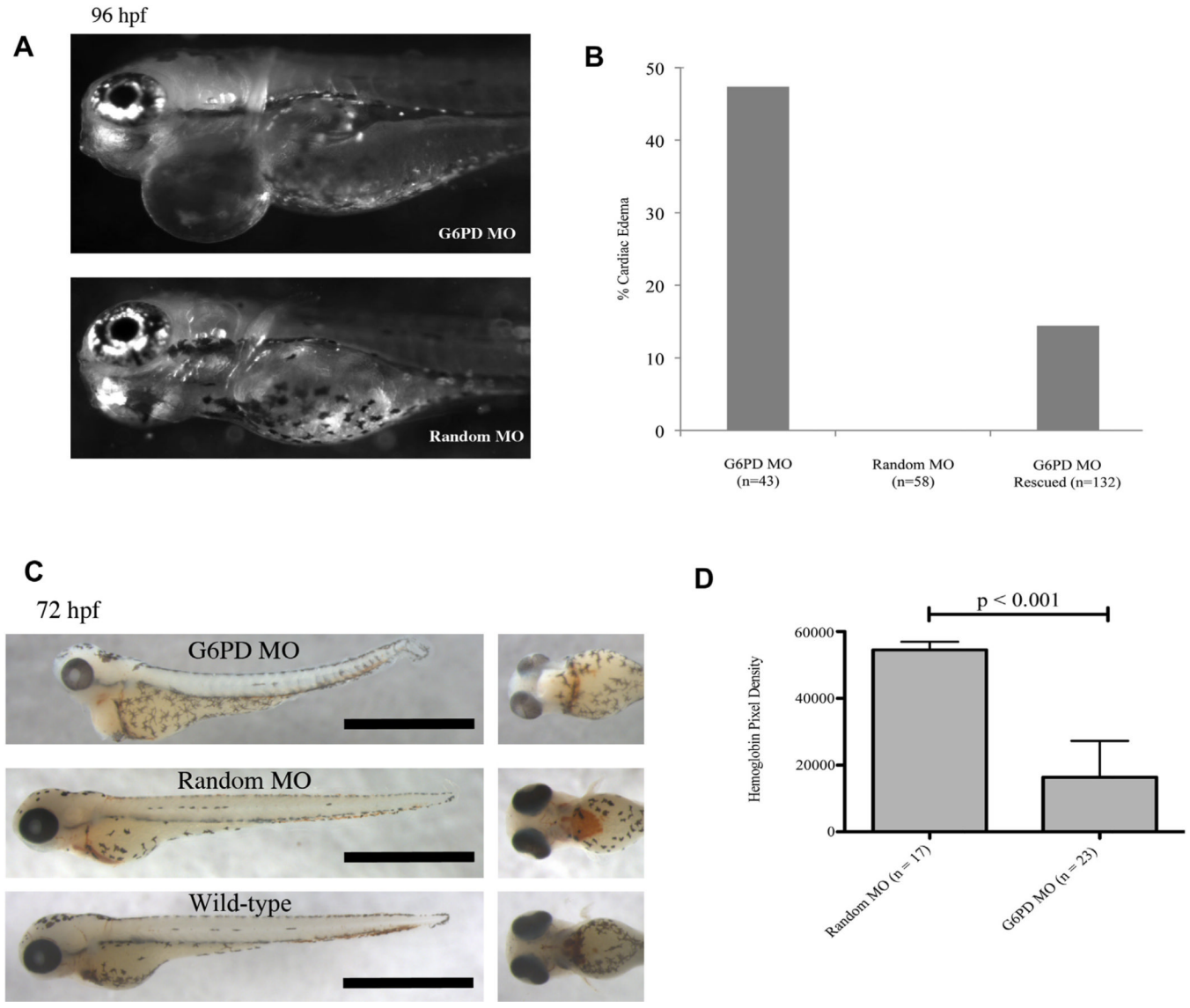

Figure 2.

Knockdown of *g6pd* in embryos produces pericardial edema and decreased hemoglobin staining. **(A)** Single-cell zebrafish embryos were injected with 1.4 pmol of random MO or 1.4 pmol of MOs targeting *g6pd*. At 96 hpf, images were taken using a Leica DMI6000B inverted microscope and a 5× objective to show significant pericardial edema. **(B)** Numbers of embryos with pericardial edema were tallied, and data were subjected to Fisher's exact test analysis for the edema phenotype in *g6pd* MO injected versus random MO injected ($p < 0.0001$). Experiments were also performed with an additional injection of 30 pg of mRNA from transcription of the *D. rerio g6pd* in rescue experiments. Fisher's exact test analysis for the edema phenotype of *g6pd* MO injected versus rescued animals showed $p < 0.0005$. **(C)** MO-injected zebrafish were stained with o-dianisidine to show hemoglobin-producing cells at 72 hpf. Scale bars represent 1000 μm. **(D)** The amount of o-dianisidine staining was quantified using ImageJ as described in the Methods section. Mean and SD are shown. The *p* value was derived using Student t test

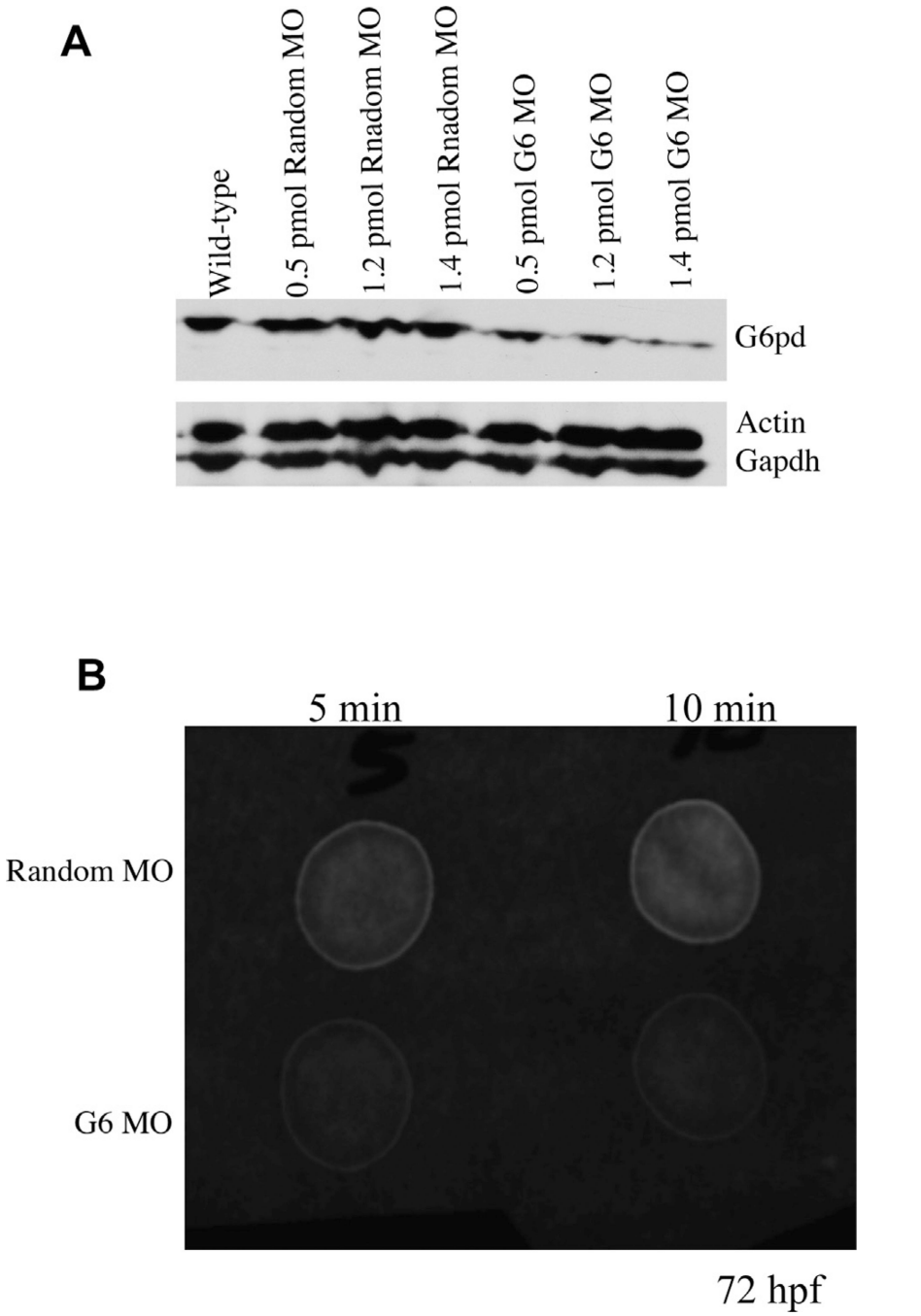

Figure 3.

Verification of MO knockdown of *D. rerio g6pd* translates to protein reduction and loss of G6pd activity. **(A)** Whole cell lysates were prepared at 72 hpf from embryos injected with different quantities of MO. Each lane represents 10 μg of protein separated by sodium dodecyl-sulfate–polyacrylamide electrophoresis followed by immunoblot using anti-G6pd antibody and appropriate secondary antibody. Detection was performed using chemiluminescence. **(B)** Whole-cell lysates of morphants were prepared, and 10 μL was used in a fluorescent G6pd activity spot assay as described previously [19]. After both 5 and 10 min of reaction time, 10 μL of reactant was spotted onto 1MM Whatman paper and

allowed to dry. Activity was determined by fluorescence of spotted reactant as viewed under a 365-nm ultraviolet light and yellow filter.

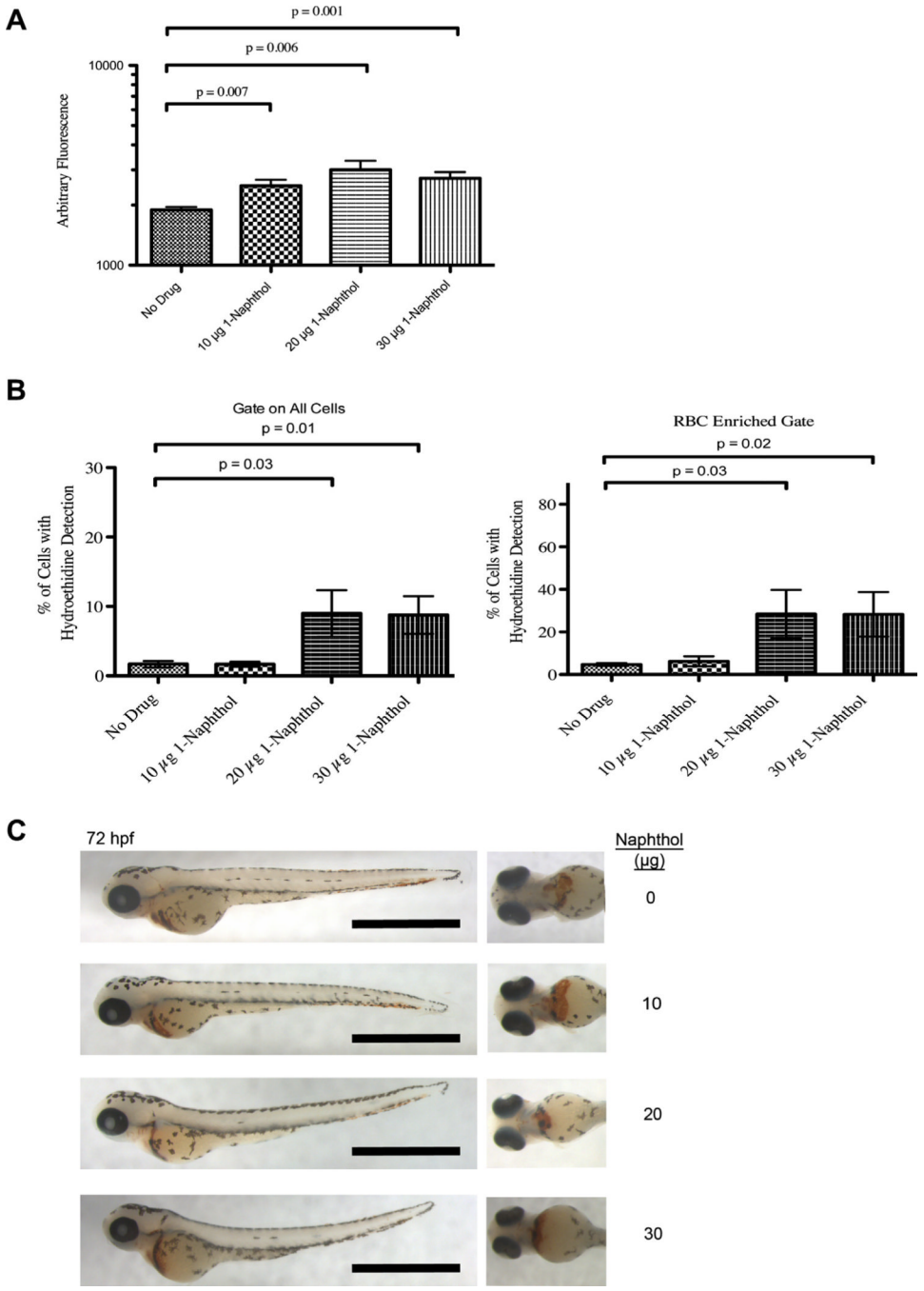

Figure 4.

1-Naphthol induced oxidative stress in zebrafish embryos. **(A)** Wild type embryos were treated from 24 to 72 hpf with increasing amounts of 1-naphthol per 5 mL of embryo water. Embryos were placed in a 96-well plate and CM-H_2DCFDA was added to 500 ng/mL. Fluorescence activity was read using 485/20 nm excitation and 528/20 nm emission on a Biotek plate reader. Shown are the mean, SEM, and *p* value derived from a Student t test (n = 21–29 embryos per group). **(B)** To determine superoxide production from embryos treated with 1-naphthol, a single-cell suspension was created and incubated with 2 μmol/L hydroethidine for 30 min. The cells were then assayed by flow cytometry with a sequential

gating strategy. First, forward and side scatter gating was performed for the total cell population. Free radical fluorescence was determined by emission capture using a 575/26-nm bandpass filter (left panel). In the same experiment, forward and side scatter gating was performed to enrich for erythrocytes, and the free radical producing fluorescence was determined as before (right panel). Shown are the mean, SEM, and *p* value derived from a Student t test (n = 6–8 embryos per group). **(C)** Increasing amounts of 1-naphthol in 5 mL of embryo water does not affect o-dianisidine hemoglobin staining in wild type embryos. Scale bars represent 1000 μm.

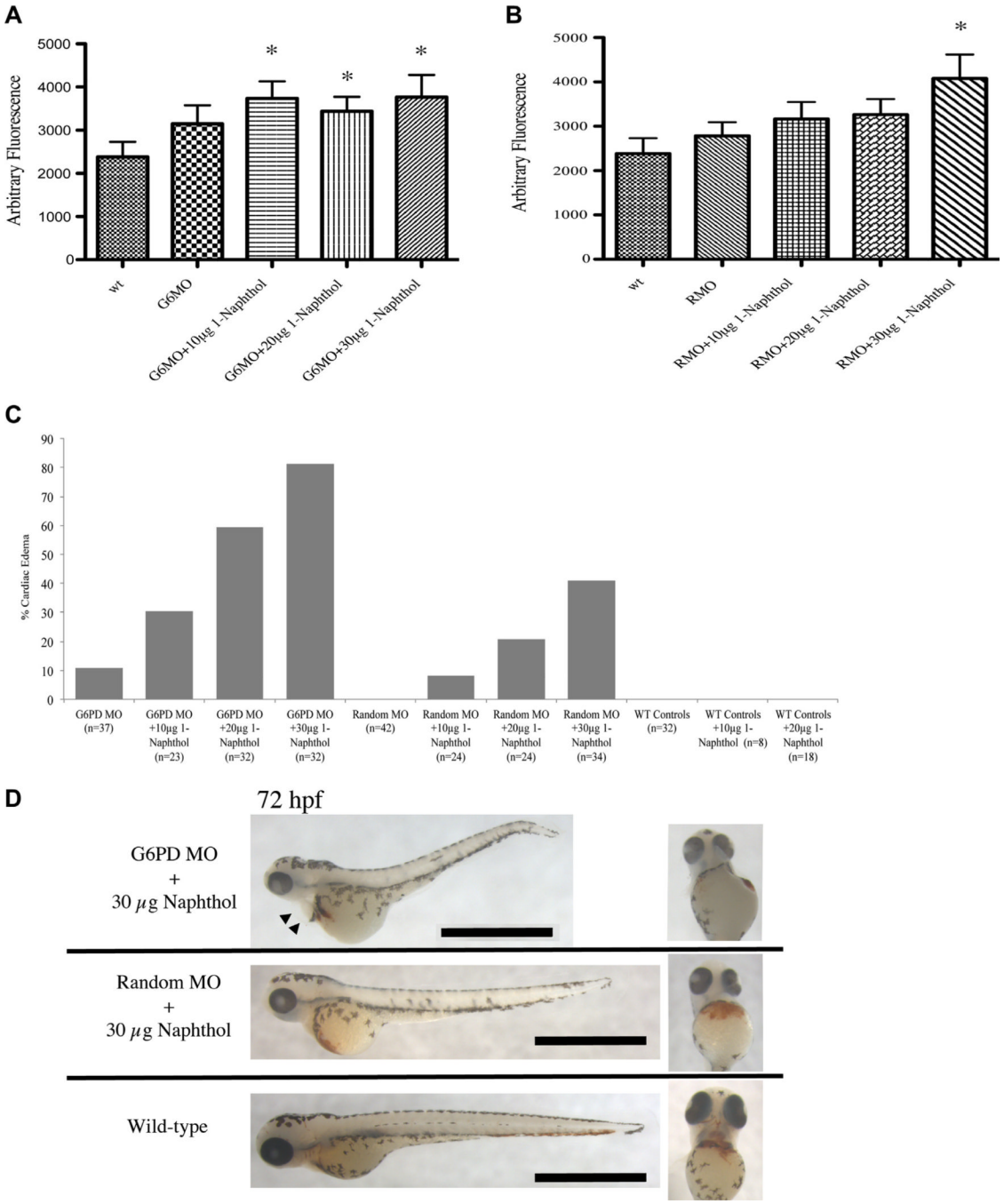

Figure 5.

1-Naphthol induces oxidative stress and edema in *g6pd* morphants. **(A, B)**Wild type embryos were injected with 1.2 pmol *g6pd* MOs or random MOs followed by exposure to increasing amounts of 1-naphthol per 5mL of embryo water from24 to 72 hpf. Embryos were placed in a 96-well plate, and CM-H_2DCFDA was added to 500 ng/mL. Fluorescence activity was read using 485/20 nm excitation and 528/20 nm emission on a Biotek plate reader. Shown are the mean and SEM (n = 21–29 embryos per group). **p* = 0.01, Student t test compared with the wild type group. **(C)** Numbers of embryos with pericardial edema were tallied after exposure to 10–30 μg 1-naphthol. Data were subjected to χ^2 analysis to

generate $p < 0.0001$. **(D)** MO-injected, 1-naphthol–treated zebrafish were stained with o-dianisidine to show hemoglobin-producing cells at 72 hpf. Black triangles indicate the extent of the pericardial edema. The scale bars represent 1000 μm.

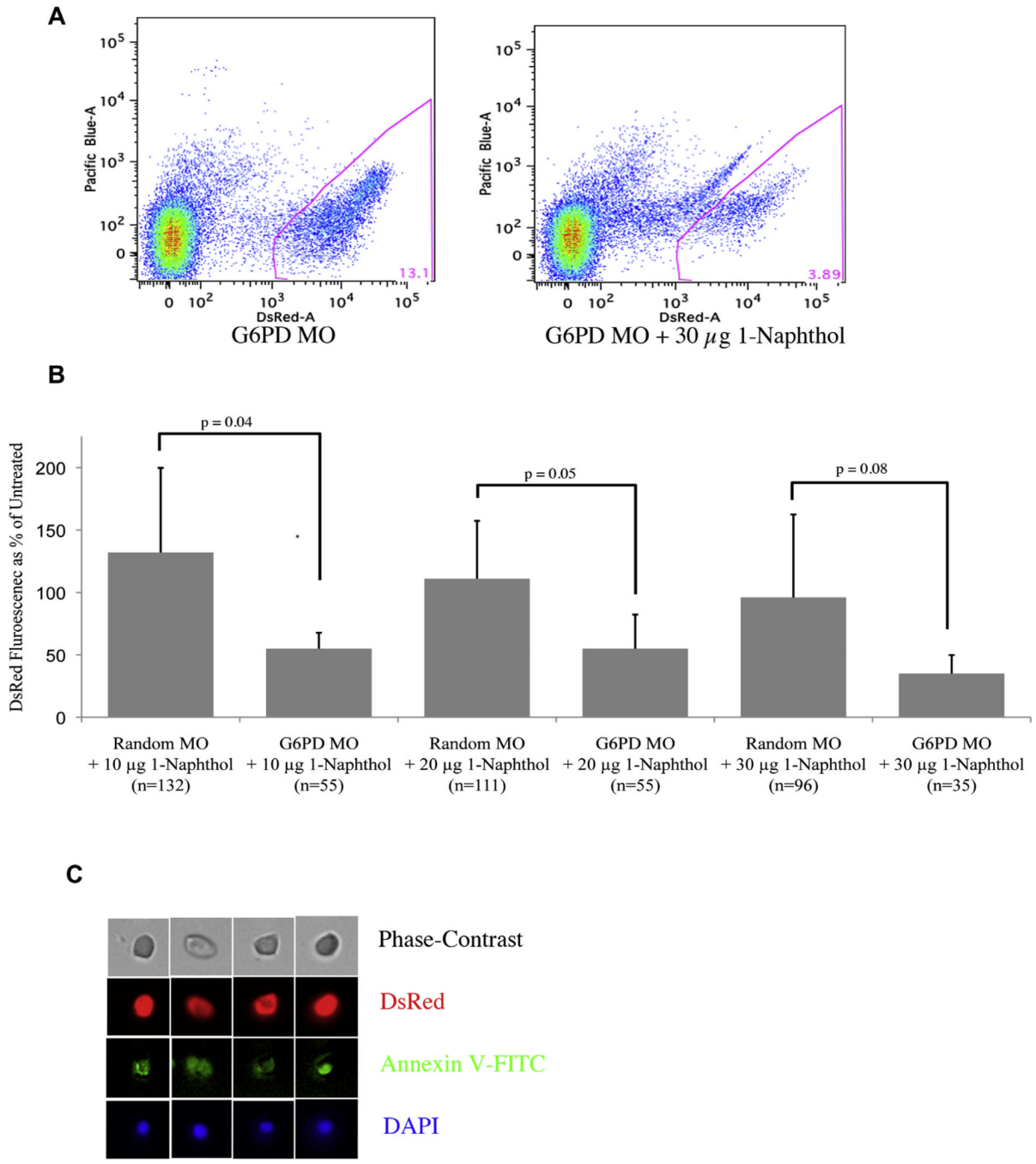

Figure 6.

1-Naphthol–induced oxidative stress causes erythrocyte apoptosis in *g6pd* morphants. **(A)** *Tg(gata1:DsRed)* embryos were injected with 1.2 pmol g6pd MO followed by 1-naphthol exposure (amounts displayed per 5 mL embryos water) from 24 to 72 hpf. A single-cell suspension was then subjected to flow cytometry to quantify the amount of DsRed-positive erythrocytes with a representative experiment shown. **(B)** Quantification of DsRed-positive erythrocytes was determined by flow cytometry at several concentrations of 1-naphthol. Data are displayed as a percent of the untreated group. Shown are the mean, SD, and *p* value derived from a Student t test (n = 3–5 experiments with 8–12 morphants per condition). **(C)**

Tg(gata1:DsRed) embryos injected with 1.2 pmol *g6pd* MO followed by 30 μg 1-naphthol exposure (per 5 mL) from 24 to 72 hpf. The single-cell suspension was stained with annexin–fluorescein isothiocyanate and nuclei stained with DAPI followed by imaging on an ImageStream flow cytometer (Amnis).

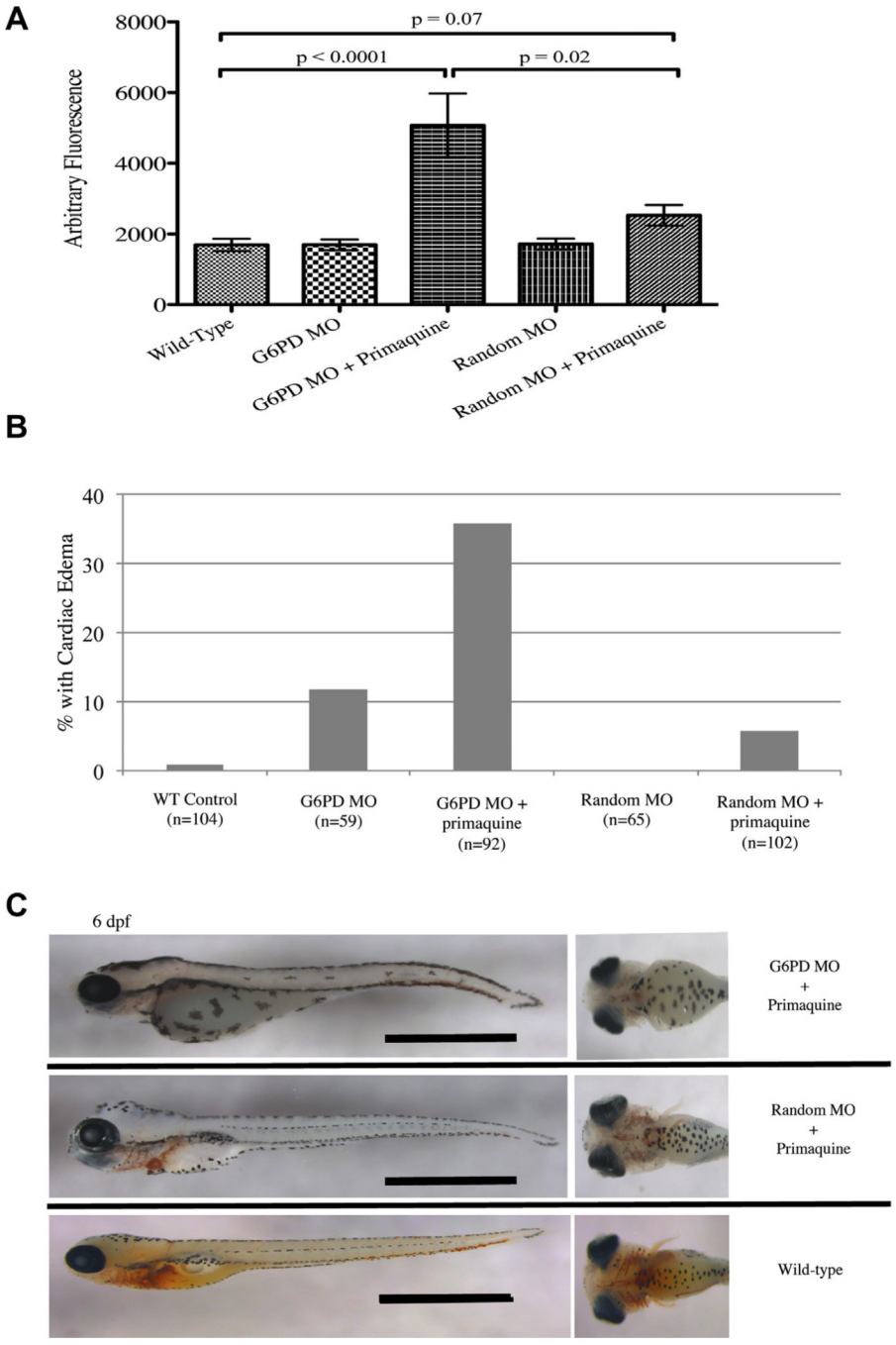

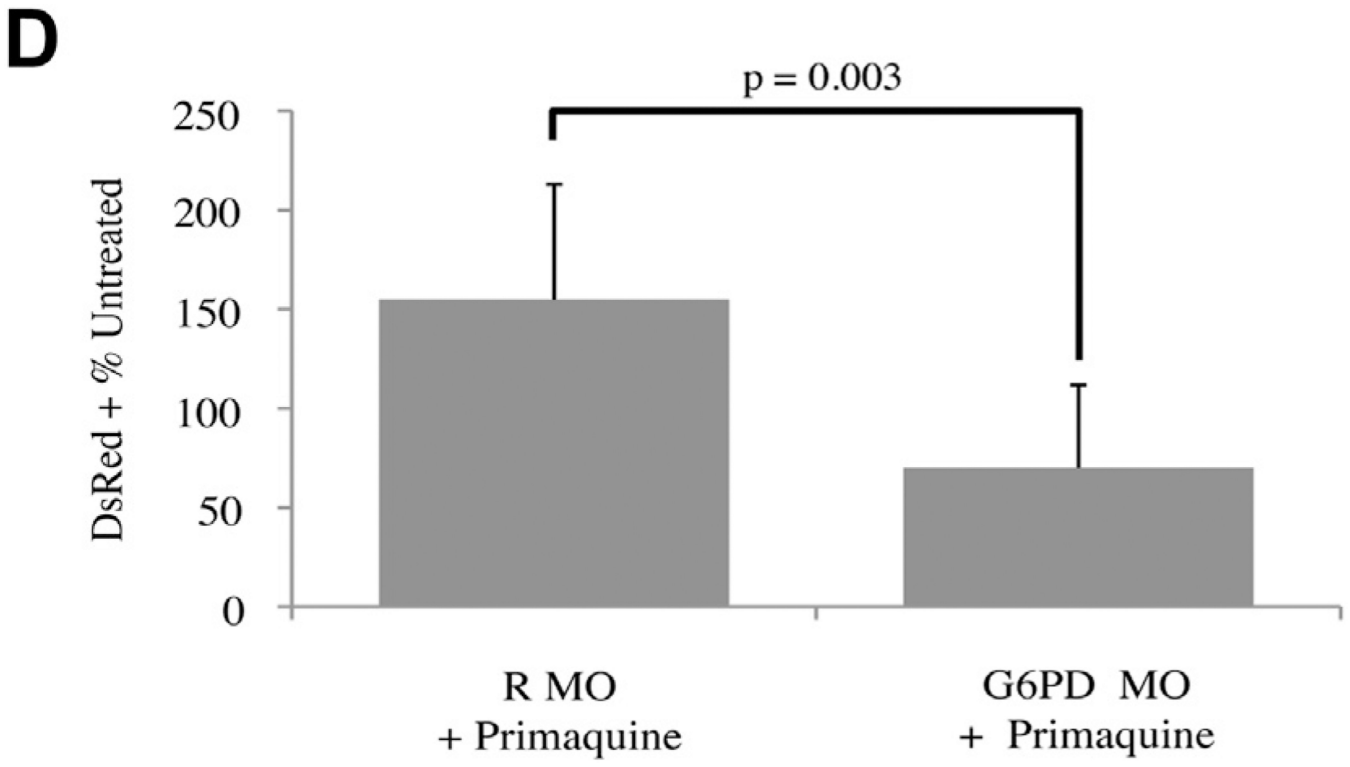

Figure 7.

Primaquine induces oxidative stress and hemolysis in *g6pd* morphants. **(A)** Wild type embryos were injected with 1.2 pmol *g6pd* MO followed by primaquine exposure of 200–250 μg per 5 mL from 24 to 144 hpf before oxidative stress measurement using a CM-H_2DCFDA fluorescence assay. Shown are the mean, SEM, and *p* value derived from a Student t test (n = 15–45 embryos per group). **(B)** Numbers of morphants with and without exposure to primaquine were assessed for pericardial edema and tallied. Data were subjected to χ^2 analysis to generate $p < 0.0001$. **(C)** Representative images from MO-injected, primaquine-exposed zebrafish that were fixed and stained with o-dianisidine to show hemoglobin-producing cells at 144 hpf. Scale bars represent 1000 μm.
(D) *Tg(gata1:DsRed)* embryos were injected with 1.2 pmol *g6pd* MO followed by (200–250 μg per 5 mL) primaquine exposure from 24 to 144 hpf. A single-cell suspension was then subjected to flow cytometry to quantify the amount of DsRed-positive erythrocytes. Shown are the mean, SD, and *p* value derived from a Student t test (n = 4 experiments with 8–10 morphants per group).